JOURNAL OF MATERIALS SCIENCE 29 (1994) 1670–1675

The relation of dynamic elastic moduli, mechanical damping and mass density to the microstructure of some glass-matrix composites

A. WOLFENDEN, J. E. GILL, V. THOMAS, A. J. GIACOMIN, L.S. COOK
Advanced Materials Laboratory, Mechanical Engineering Department, Texas A&M University, College Station, TX 77843-3123, USA

K. K. CHAWLA, R. VENKATESH
Department of Materials and Metallurgical Engineering, New Mexico Institute of Mining and Technology, Socorro, NM 87801, USA

R.U. VAIDYA
Los Alamos National Laboratory,MST-5, MS E 546, Los Alamos, NM 87545, USA

Dynamic elastic moduli and mechanical damping were measured with the PUCOT (piezoelectric ultrasonic composite oscillator) technique at room temperature for ceramic-matrix composites (CMCs) of the following compositions: PRD-166 (fibres)/N51A glass (matrix), PRD-166 fibres coated with SnO_2/glass, Nextel 480 fibres/glass, Nextel 480 fibres coated with SnO_2/glass, and Nextel 480 fibres coated with BN/glass. The fibres were continuous, and the volume fractions varied from 0.24 to 0.43. Some of the mechanical-property measurements correlated with the thickness of one of the coating materials, and with microstructural observations of the misorientation angle of the fibres and normalized fibre length. With increasing volume fractions of fibres, the fraction of broken fibres increased. For the PRD-166/glass and PRD-166/SnO_2/glass, a substantial fraction of the fibres were misoriented by angles of up to 15°. Assessments were made of the measured properties in terms of the rule of mixtures and other theoretical estimations.

1. Introduction

The successful use of advanced ceramic materials in structural applications hinges on improving the confidence that designers have in the reproducibility of the physical and mechanical properties of these materials. In particular, some modern research in materials science focuses on improving the fracture toughness of ceramics by incorporating various kinds of fibres to form ceramic-matrix composites (CMCs) [1–6]. It is desirable to have ceramics that can tolerate several stress states (not merely compression), relatively rapid changes in temperature, and impacts, thus permitting a wider variety of service conditions. A promising approach to solving the problem of the low fracture toughness of CMCs involves coating the reinforcing fibres.

Such a coating functions as a barrier to prevent chemical interaction at the fibre/matrix interface, and it prevents strong interfacial chemical bonding. This weak fibre/coating or coating/matrix interface induces various toughening mechanisms in CMCs, including crack deflection, and/or fibre debonding, and fibre pull-out. We have used this interface engineering approach (involving fibre coating, characterization of the fibre strength after coating and of the microstructure of the interface, thermal-stress analysis, mechanical testing and fractographic studies) with the alumina fibre/silica-based glass and mullite/glass systems to weaken the interfacial bond so as to achieve oxide/oxide composites with strong, tough behaviours [4, 7–10].

An important mechanical property for characterizing the mechanical behaviour of such composites is the elastic modulus. In this paper we report measurements of the dynamic Young's modulus, the dynamic shear modulus and mechanical damping (internal friction) performed with the PUCOT (piezoelectric ultrasonic composite oscillator) technique, and of mass density, for CMCs with glass as the matrix and with two kinds of continuous ceramic fibres as the reinforcement. Some of the fibres were coated with SnO_2 or BN. It is shown that some of these measurements can be correlated with the thickness of one of the coating materials, and with microstructural observations of the misorientation angle of the fibres and the normalized fibre length.

2. Experimental procedure

2.1. Specimen fabrication

N51A borosilicate glass was used as the matrix

0022–2461

TABLE I Composition of N51A glass matrix (from Owens Illinois Inc., USA)

Compound	Composition (wt %)	Element	Composition (at %)
SiO_2	72	Si	33.6
B_2O_3	12	B	3.8
Al_2O_3	7	Al	3.7
CaO	1	Ca	0.7
Na_2O	6	Na	4.5
K_2O	2	K	1.7
BaO	< 0.1	Ba	Trace
		O_2	Balance

material in fabricating all the composite specimens. The composition of this glass is given in Table I. Two different kinds of continuous fibres – PRD-166 (α-alumina with 15–20 wt % zirconia) from DuPont and Nextel 480 (70 wt % alumina + 28 wt % silica + 2 wt % boria) from the 3 M Company – were employed. Tin dioxide was used as the coating material with the PRD-166 fibres, while boron nitride was used as the coating for Nextel fibres. Both coatings were deposited on the fibre surfaces by chemical vapour deposition (CVD). The average thickness of the SnO_2 coating was 1 μm, while the average thicknesses of the BN coatings were 0.1, 0.2 or 0.3 μm. The volume fractions of the fibres, V_f, were in the range 0.24 to 0.43.

Specimen fabrication was by the slurry-infiltration technique. A slurry of the glass powder in an organic binder was produced, and the fibres were drawn through the slurry. These fibre tows were then dried, cut and stacked, and the binder burnout process was at 500 °C. After binder burnout, the stacks were wrapped in a graphite foil and hot pressed in a graphite die at 925 °C and 3 MPa for 15 min. Fig. 1 shows a schematic diagram of the specimen-preparation process. In total, nine different CMCs were produced. Specimens of suitable size for the PUCOT and density measurements, and for microstructural observations, were cut with a low-speed diamond cut-off saw.

2.2. Mass-density measurements

The Archimedes technique (with water) was used to determine the mass density, ρ, of the specimens at room temperature. The value of the density for distilled water at 4 °C was used as a reference. Corrections were made for changes in the density of water with temperature.

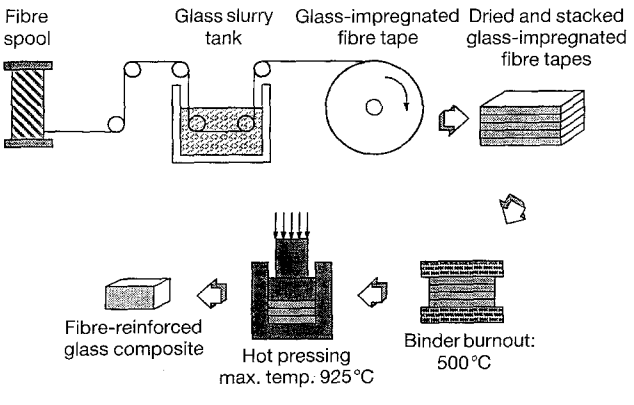

Figure 1 A schematic diagram of the specimen-preparation process.

2.3. Measurements of dynamic elastic moduli and damping

The PUCOT technique [11–15] was used at frequencies in the range 40–100 kHz to measure the dynamic Young's modulus, E, the dynamic shear modulus, G, the longitudinal strain amplitude, the torsional strain amplitude and the mechanical damping, Q^{-1}, for parallelepipedal specimens cut to appropriate resonant lengths. In the case of the torsional measurements, corrections to the values of the shear modulus were made to account for the non-circular symmetry of the specimens [16].

2.4. Determination of fibre misorientation and normalized fibre length

Optical and scanning electron microscopy were used for general characterization of the microstructure of the composites. Optical microscopy was used to evaluate the volume fraction of the fibres and the fibre distribution in the composites. Samples were cut on a diamond saw, mounted in epoxy, and then they were ground and polished. Final polishing was done with 0.1 μm diamond paste. Fibre volume fractions were evaluated by the lineal-intercept method.

The hot-pressing step in the slurry-impregnation process of making continuous fibre-reinforced-glass-matrix composite can result in two types of damage: (a) fibre misalignment, and (b) fibre breakage. To examine the extent of the damage, we polished the samples, examined them by scanning electron microscopy (SEM), and measured the fibre lengths and misorientation from the zero-degree (axial) line. To reveal the fibres more clearly, the surface of the composite was lightly etched with HF. For each sample, 200–300 fibres were studied. Fibres which ran the whole length of the micrographs were taken to be unbroken.

3. Results and discussion

The results from the mass-density measurements and from the PUCOT measurements are displayed in Table II; also shown are the values of the volume fraction of the fibres, V_f, the coating thicknesses, the experimental and theoretical Young's modulus, E, the damping, Q^{-1}, in the longitudinal mode, the theoretical and experimental mass density, ρ, experimental and theoretical shear modulus, G, and the experimental damping in the torsional mode for the CMCs. In Table II, the values of G_{theo} are calculated from [17]:

$$G_{theo} = G_m + \frac{V_f}{(A + B)} \quad (1)$$

where $A = 1/(G_f - G_m)$ and $B = (1 - V_f)/2G_m$. Some assumptions have been made in this computation:

TABLE II Volume fraction of fibre, coating thicknesses, experimental and theoretical values of Young's modulus, experimental values of damping in the longitudinal mode, theoretical and experimental values of the mass density, experimental and theoretical values of the shear modulus and experimental values of damping in the torsional mode for the CMCs

Sample number	V_f	Coating thickness (μm)	E_{expt} (GPa)	E_{theo} (GPa)	$E_{p,corr}$ (GPa)	Q^{-1} longitudinal	ρ_{theo} (kg m^{-3})	ρ_{expt} (kg m^{-3})	G_{expt} (GPa)	G_{theo} (GPa)	Q^{-1} torsional
1[a]	0.29	0.0	108	115	107	0.0016	2447	2525	38	38	0.0018
2[b]	0.29	0.2	95	115	107	0.0003	2447	2481	37	38	0.0011
3[c]	0.43	0.0	177	204	192	0.0031	3060	3016	48	52	0.0022
4[c]	0.25	0.0	137	149	140	0.0022	2700	2730	42	40	0.0009
5[d]	0.36	1.0	146	183	172	0.0009	2920	2851	40	46	0.0009
6[b]	0.29	0.3	103	115	107	0.0009	2447	2480	34	38	0.0080
7[d]	0.24	1.0	128	146	137	0.0006	2680	2728	38	39	0.0009
8[e]	0.29	0.2	91	115	107	0.0007	2447	2455	36	38	0.0025
9[b]	0.29	0.1	88	115	107	0.0008	2447	2450	31	38	0.0010

[a] Nextel 480/glass (uncoated).
[b] Nextel 480/BN/glass (coated).
[c] PRD-166/glass (uncoated).
[d] PRD-166/SnO_2/glass (coated).
[e] Nextel 480/SnO_2/glass (coated)
$E = E_{matrix} = 72$ GPa, E_f(PRD-166) = 380 GPa, E_f(Nextel 480) = 221 GPa, $E(SnO_2)$ = 233 GPa, E(BN) = 60 GPa. $E_{p,corr}$ is the Young's modulus corrected for porosity. E_{theo} is E from the rule of mixtures (ROM). G_{theo} is from the method of reference [17]. The literature shows values of Young's modulus for BN to be 50–200 GPa. However, the amount of BN, in terms of the volume fraction of the total composite, is negligible. Therefore, the contribution of BN to the elastic modulus of the composite is insignificant. The coating thicknesses are average values.

namely, the components are isotropic materials, the values of G for the fibre, fibre and coating, and the glass matrix were evaluated using $G = [E/2(1 + PR)]$, where PR is Poisson's ratio (assumed to be 0.25); in the case of the SnO_2-coated PRD-166 CMCs, appropriate volume fractions of the coating were evaluated using a coating thickness of 1 μm; and in the Nextel 480/glass system the BN and SnO_2 coatings were ignored because of their insignificant amounts. The experimental and theoretical values of the Young's modulus and the shear modulus are presented graphically as functions of the fibre volume fraction in Figs 2 and 3.

From the data on densities given in Table II, we note that the agreement between the values of ρ_{theo} and ρ_{expt} is remarkably good; that is, the ratios fall between 0.97 and 1.02. Some of the deviation from unity is likely to be due to the errors in the measurement of porosity in the specimens. The porosity, as evaluated by image analysis, was approximately 3–4%.

Also, from the data displayed in Table II and in Fig. 2, we can see that the experimental values of the Young's modulus of the uncoated specimens of the PRD-166/glass system are smaller than the theoretical rule-of-mixtures (ROM) value, as expected. It should be noted, however, that the lack of a fibre coating in these uncoated-fibre composites leads to chemical reactions between the matrix and the fibre. In the calculations, the effect of the reaction products is not taken into account. Hence, the ROM equation is not likely to be accurate in such a situation. Moreover, there are also likely to be effects due to fibre breakage and fibre misorientation.

For the SnO_2-coated PRD-166 CMCs, the experimental values of Young's modulus are also lower than those predicted by the ROM. For both the PRD-

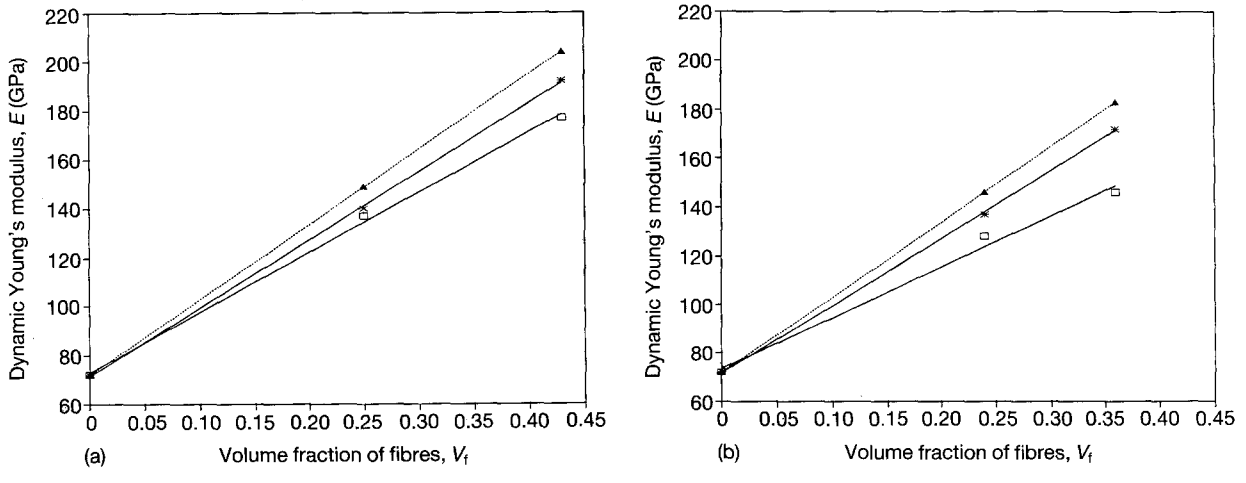

Figure 2 (—□—) Experimental and (··· ▲ ···) theoretical values, with the correction (— × —) for porosity, of Young's modulus as a function of the fibre volume fraction: (a) for PRD-166/glass, and (b) for PRD-166/SnO_2/glass.

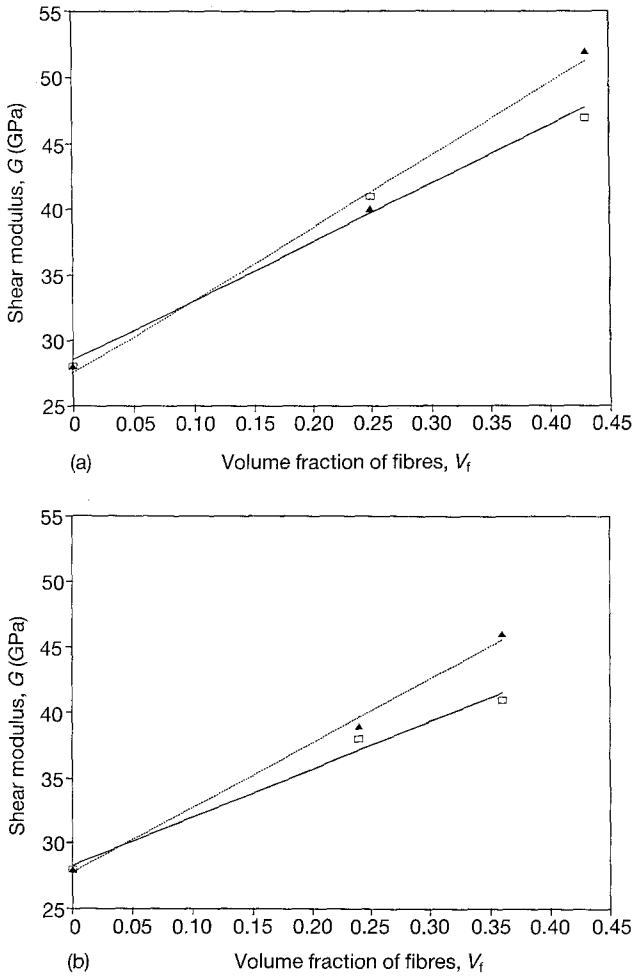

Figure 3 (—□—) Experimental and (··· ▲ ···) theoretical values of the shear modulus as a function of the fibre volume fraction: (a) for PRD-166/glass, and (b) for PRD-166/SnO_2/glass.

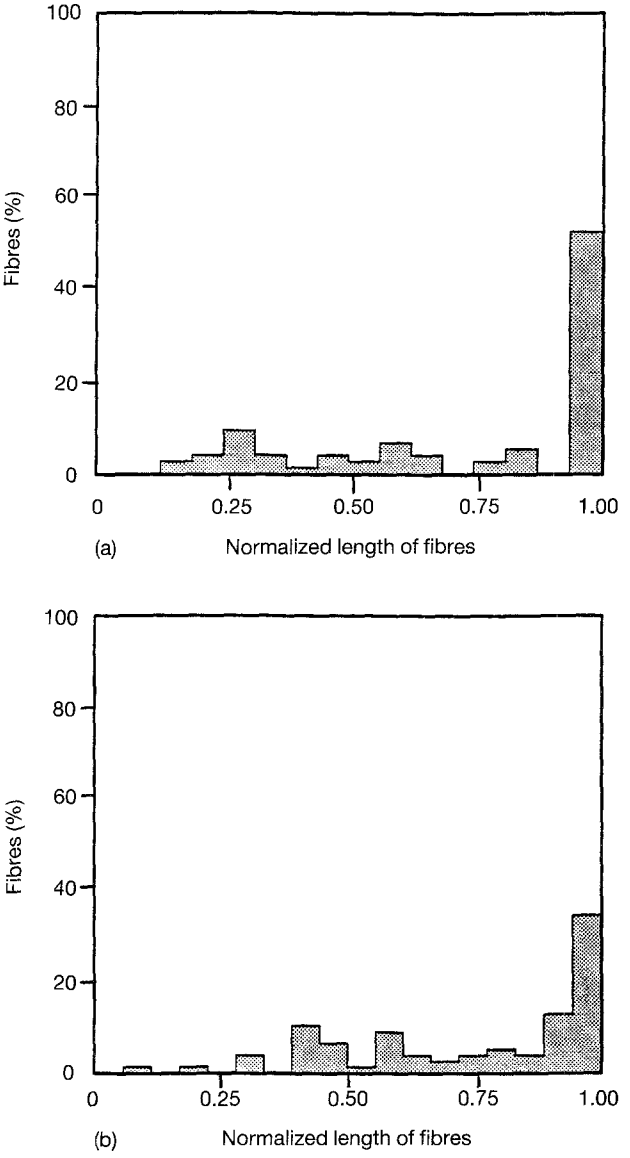

Figure 4 Normalized fibre-length distribution in PRD-166/glass CMCs: (a) volume fraction = 0.25, and (b) volume fraction = 0.4.

166/glass systems (coated or uncoated fibres) the values of Young's modulus and shear modulus increase as the volume fraction of the fibres increases, as expected.

With increasing volume fractions of the fibres, the fraction of broken fibres increases, as can be seen from an inspection of Figs 4 and 5. From the data in Table II, we note that $\Delta E(= E_{theo} - E_{expt})$ increases as V_f increases. This reflects the effects of porosity and fibre breakage on the elastic modulus of the composite.

Regarding the Nextel 480/glass system, an inspection of the data in Table II reveals that the experimental values of Young's modulus are consistently lower than the theoretical (ROM) values, as anticipated, and that the values of E_{expt} are much closer to the values of $E_{p,corr}$. The presence of the 0.2 μm of SnO_2 on the Nextel 480 fibres appears to lower the Young's modulus of the composite, implying that the integrity of the coating is not perfect. Further, in the Nextel 480/SnO_2/glass system, there are reaction products at the interface. The Nextel fibre contains SiO_2, which has a limited reaction with SnO_2. This reaction probably causes degradation of the fibre, which would enhance separation of the fibre from the matrix, and thus lower the elastic modulus of the composite. The same observation occurs for the case of the BN-coated Nextel 480 fibres where it is seen that with an average coating thickness of 0.1 or 0.2 μm, the values of the Young's modulus for the composite are reduced from 108 to 88 or 95 GPa, respectively, while the value of E_{expt} for the specimen containing fibres coated with BN of thickness 0.3 μm is 103 GPa; this is essentially equal to the value for the uncoated specimen (108 GPa). For these specimens with BN-coated Nextel 480 fibres, clean debonding and pull-out were observed only in the case of the 0.3 μm thick coating. Thus, the integrity of the 0.1 μm and 0.2 μm BN coatings also appears to be imperfect, while that of the 0.3 μm BN coating appears to be good. In this respect, it is noteworthy that specimen numbers 2 and 8, with BN and SnO_2 coatings, respectively, and with the same fibre volume fraction and the same coating thickness, had values of E and G that were essentially the same, and that the values of E were less than the value of E for the specimen with no coating.

For both systems studied, the values of G_{expt} and G_{theo} agree with each other to better than 18%, as can be seen in Fig. 3. For the Nextel 480/glass system, the experimental values of the shear modulus are essentially constant at 35 ± 3 GPa.

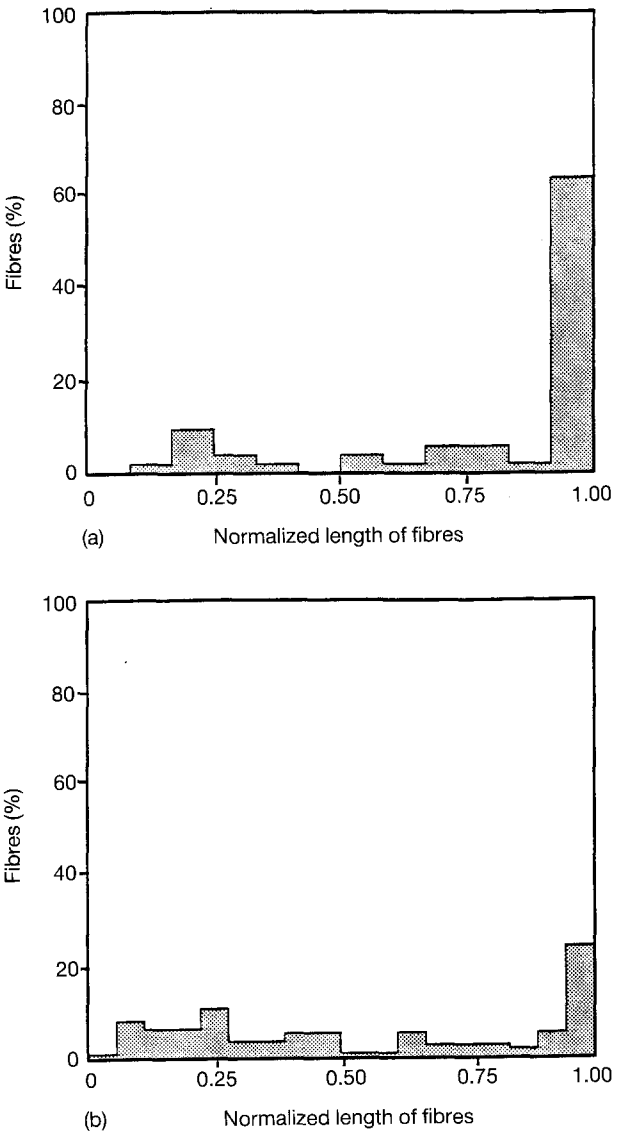

Figure 5 Normalized fibre-length distributions in PRD-166/SnO_2/glass CMCs: (a) volume fraction = 0.24, and (b) volume fraction = 0.4.

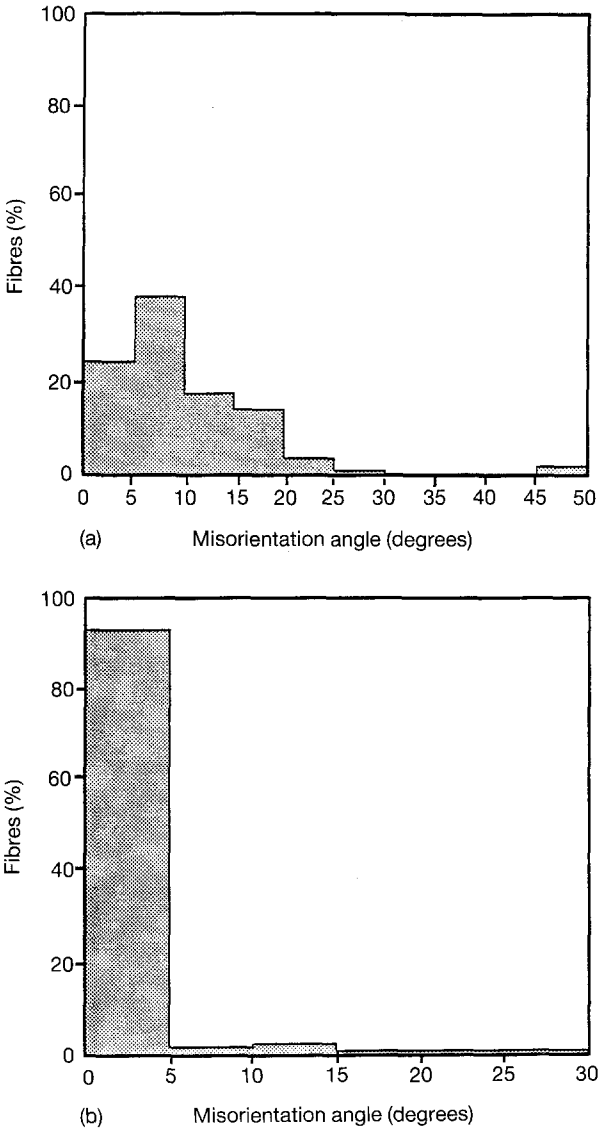

Figure 6 Fibre misorientation distribution in PRD-166/glass CMCs: (a) volume fraction = 0.25, and (b) volume fraction = 0.4.

From the damping data in Table II, it can be seen that for the longitudinal mode the values lie between 0.0003 and 0.0031, while for the torsional mode they are between 0.0009 and 0.0080. It must be realized that, with the PUCOT, the reproducibility of damping values for multiple tests on a single specimen is typically to within a factor of 2 to 4 [12, 13], even with specimens with simple microstructures such as fused quartz or quartz single crystals. Hence, the variations in damping in Table II are likely to be the result of variations in reproducibility, rather than real effects due to changes in the fibre volume fraction or the coating thickness. However, we can confirm that the mean level of longitudinal damping for the specimens studied was 1.2×10^{-3}, with a standard deviation of 0.9×10^{-3}. For the torsional mode, the mean damping was 2.1×10^{-3} with a standard deviation of 2.3×10^{-3}. These levels of damping are typical for ceramics.

The effect of fibre misorientation and breakage on the Young's modulus of unidirectional composites is given in [1]. For a carbon-fibre/epoxy-matrix composite, the elastic modulus in the longitudinal direction can decrease by as much as 15% for a fibre misorientation of 5°, and by as much as 60% for a fibre misorientation of 15°. Figs 6 and 7 for the PRD-166/glass and PRD-166/SnO_2/glass composites, respectively, indicate that a substantial fraction of the fibres are misoriented by angles up to 15°. However, determination of the effect of the fibre misorientation on the Young's modulus of the composites requires determination of quantities such as the transverse elastic modulus, Poisson's ratio and the shear modulus. For our specimens, only the values of the shear modulus are available, and hence we cannot proceed with this determination. Empirical efficiency factors for the fibre misorientation, η_θ and fibre length, η_1, can be incorporated into the ROM as [18]

$$E_c = E_m V_m + \eta_\theta \eta_1 E_f V_f \quad (2)$$

Another possible cause for the discrepancy between the theoretical and the experimental values of the Young's modulus is the porosity in these CMCs. Porosity can reduce the elastic modulus significantly,

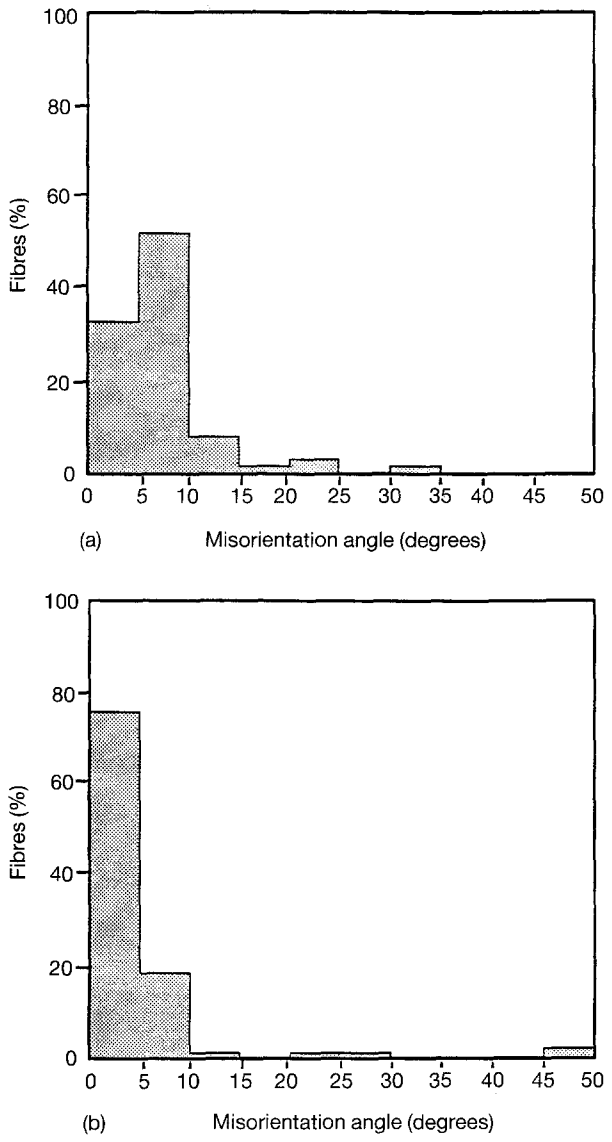

Figure 7 Fibre misorientation distribution in PRD-166/SnO_2/glass CMCs: (a) volume fraction = 0.24, and (b) volume fraction = 0.4.

and its effect on the Young's modulus can be described by Mackenzie's equation [19].

$$E_{p,corr} = E_{co}(1 - bV_p - b_1V_p^2) \quad (3)$$

where $E_{p,corr}$ is the Young's modulus of the composite with a volume-fraction of porosity of V_p, E_{co} is the elastic modulus of the composite with zero porosity, and b and b_1 are constants related to the material. For most materials, $b = 2$ and $b_1 = 0.5$. With this equation, and taking $E_{co} = E_{theo}$, one finds that these calculated values of the elastic modulus, $E_{p,corr}$, for the composites, which had 3–4% porosity, are closer to the experimental values.

4. Conclusions

From this experimental study of the mass density, elastic moduli and mechanical damping for the PRD-166/glass and Nextel 480/glass CMCs, we can make the following conclusions.

1. For both types of CMCs, as the volume fraction of fibres increased, the fraction of broken fibres increased.

2. For the PRD-166/glass and PRD-166/SnO_2/glass composites, a substantial fraction of the fibres were misoriented by angles up to 15°.

3. The agreement between the theoretical and experimental values of the mass density is such that their ratios fall between 0.97 and 1.02. Some of the deviation from unity is likely to be due to errors in the measurement of the porosity in the specimens.

4. In the PRD-166/glass systems (both for coated or uncoated fibres), the values of the Young's modulus and the shear modulus increased as the volume fraction of the fibres increased, as expected.

5. The experimental values of the Young's modulus of the coated or uncoated specimens of the PRD-166/glass system were smaller than the theoretical values obtained by the ROM.

6. In the Nextel 480/glass system, the experimental values of the Young's modulus were consistently lower than the theoretical (ROM) values, as anticipated, and the values of E_{expt} were much closer to the values of $E_{p,corr}$.

7. For both the systems studied, the values of G_{expt} and G_{theo} agreed with each other to better than 18%. For the Nextel 480/glass system, the experimental values of the shear modulus were 35 ± 3 GPa.

8. The mean level of damping for the specimens studied was near to 10^{-3}, which is a typical value for ceramics.

References

1. K. K. CHAWLA, "Composite materials: science and engineering" (Springer-Verlag, New York, 1987) p. 134.
2. K. M. PREWO, J. J. BRENNAN and G. K. LAYDEN, *Ceram. Bull.* **65** (1986) 305.
3. D.C. PHILLIPS, *J. Mater. Sci.* **9** (1972) 1847.
4. A. MAHESHWARI, K. K. CHAWLA and T. A. MICHALSKE *Mater. Sci. Engng. A* 107(1969) 269.
5. T. A. MICHALSKE and J. HELLMANN, *J. Amer. Ceram. Soc.* **71** (1988) 725.
6. A. G. EVANS, *Mater. Sci. Engng.* **A 107** (1969) 227.
7. R. VENKATESH and K. K. CHAWLA, *J. Mater. Sci. Lett.* **11** (1992) 650.
8. J. -S. HA and K. K. CHAWLA, *ibid.* **12** (1993) 87.
9. K. K. CHAWLA, M. K. FERBER, Z. R. XU and R. VENKATESH, *Mater. Sci. Engng* **A 162** (1993) 35.
10. R. U. VAIDYA, J. A. FERNANDO, K. K. CHAWLA and M. K. FERBER, *ibid.* **A 151** (1992) 161.
11. J. MARX, *Rev. Sci. Instrum.* **22** (1951) 503.
12. W. H. ROBINSON and A. EDGAR, *IEEE Trans. Son. Ultrason.* **21** (1974) 98.
13. A. WOLFENDEN and W. H. ROBINSON, *Scripta Metall.* **10** (1976) 763.
14. V. THOMAS, A. J. GIACOMIN and A. WOLFENDEN, *Rev. Sci. Instrum.* **64** (1993) 492.
15. W. H. ROBINSON, S. H. CARPENTER and J. L. TALLON, *J. Appl. Phys.* **45** (1974) 1975.
16. S. SPINNER and W. E. TEFFT, *Proc. ASTM* **61** (1961) 1229.
17. K. WAKASHIMA and H. TSUKAMOTO, *ISIJ Int.* **32** (1992) 883.
18. V. LAWS, *J. Phys. D: Appl. Phys.* **4** (1971) 1737.
19. J. K. MACKNENZIE, *Proc. Phys. Soc. (London)* **B 63** (1950) 2.

Received 5 May
and accepted 18 August 1993